

---

# Studies on Synthesis and Electrochemical Properties of Lithium Ferrous Silicate Cathode Materials

Wang Qingsheng<sup>1,2</sup>, Pavel Novikov<sup>1,2</sup>, Anadoli Popovich<sup>2</sup>, Yang Zhelong<sup>1</sup>, Yu Yao<sup>1</sup>, Okonov Leonid<sup>2</sup>

<sup>1</sup>Technology Department, Zhejiang Changxing Sino-Russian Institute of New Energy Materials Technology, Changxing, China

<sup>2</sup>Technology Department, Peter the Great Polytechnic University, St. Petersburg, Russia

## Email address:

tse-battery@mail.ru (Wang Qingsheng), novikov.p.a@gmail.com (P. Novikov)

## To cite this article:

Wang Qingsheng, Pavel Novikov, Anadoli Popovich, Yang Zhelong, Yu Yao, Okonov Leonid. Studies on Synthesis and Electrochemical Properties of Lithium Ferrous Silicate Cathode Materials. *Advances in Materials*. Vol. 11, No. 1, 2022, pp. 20-29.

doi: 10.11648/j.am.20221101.13

**Received:** December 15, 2021; **Accepted:** December 25, 2021; **Published:** March 23, 2022

---

**Abstract:** The lithium ferrous silicate ( $\text{Li}_2\text{FeSiO}_4$ ) has high theoretical capacity of 330 mAh/g, abundant raw material resources, stable working voltage, excellent thermal stability of Si-O bond, environmental protection and low cost, and has become one of the attractive cathode materials in high-energy lithium batteries. However, the conductivity of  $\text{Li}_2\text{FeSiO}_4$  material itself is poor, and the ionic conductivity is low, so improving the conductivity and  $\text{Li}^+$  diffusion coefficient of the material has become the focus of research. In this paper,  $\text{Li}_2\text{FeSiO}_4$  material was synthesized by the combination of sol-gel method and solid-state sintering method, and the nano-material and metal ion doping were realized by liquid-phase grinding method, which increased the specific surface area and conductivity of the material and increased the specific energy of the material. XRD, TGDSC, particle size analysis and electrochemical capacity test show that the specific capacity of the initial  $\text{Li}_2\text{FeSiO}_4$  material synthesized in solid phase is 120 mAh/g, and the capacity of the nano-treated  $\text{Li}_2\text{FeSiO}_4$  material reaches 140mah/g; The  $\text{Li}_2\text{Fe}_{0.5}\text{Mn}_{0.5}\text{SiO}_4$  material obtained by Mn doping has a capacity of 160mah/g; The volume of  $\text{Li}_2\text{Fe}_{0.5}\text{Mn}_{0.45}\text{Ti}_{0.05}\text{SiO}_4$  synthesized by adding metal Ti is increased to 195mah/g; The electrical conductivity of  $\text{Li}_2\text{Fe}_{0.5}\text{Mn}_{0.5}\text{Si}_{0.975}\text{V}_{0.025}\text{O}_4+\text{C}$  synthesized by doping v and c can be significantly improved, and the discharge capacity can reach about 200mAh/g. In the liquid phase grinding of the mixture of ethanol and acetone, it was found that the tautomers of alcohol and ketone were in the dynamic equilibrium of ketone and enol, and acetone met positively charged metal ions to form stable metal salts, which improved the stability of the material.

**Keywords:** Lithium Ferrous Silicate, Solid Phase Synthesis, Nanocrystallization, Liquid Phase Grinding, Ketoenolic Dynamic Equilibrium, Metal Ion Doping

---

## 1. Preface

In recent years, with the introduction of carbon-neutral and peak carbon dioxide emissions policies, the environmental protection requirements have become more and more strict, and the country is vigorously promoting and advocating low-carbon policies. Traditional energy raw materials, such as coal and oil, are non-renewable resources, and will also have adverse effects on the environment after use, such as acid rain, global warming, etc., which seriously affects our living environment, so we should use less fossil fuels as much as possible and use more renewable or clean energy, such as photovoltaic energy, wind energy, tidal energy and so on [1]. In order to expand the use

range of green energy, further improve the utilization rate of energy and reduce pollution, clean energy vehicles with lithium ion energy storage batteries as the power source came into being [2]. Among the power systems in use recently, according to the comprehensive evaluation results of their cost performance by researchers, it is generally believed that secondary chemical power is the most competitive energy carrier for mobile power [3]. From lead-acid battery to nickel-hydrogen battery, and now the lithium-ion battery which is widely used in the market has been the main body of mobile power supply. Among them, with the continuous improvement of its performance, the technical level of lithium-ion battery is also developing by leaps and bounds, especially the research on improving the energy density of the cathode material of lithium-ion battery has been in

progress. Recently, our hospital has conducted a more in-depth study on  $\text{Li}_2\text{FeSiO}_4$ , and achieved the expected results. The  $\text{Li}_2\text{FeSiO}_4$  has a high theoretical capacity of 330 mAh/g, and theoretically two lithium ions can be deintercalated, but the ionic conductivity of  $\text{Li}_2\text{FeSiO}_4$  itself is very low. Therefore, around

the above problems, this paper adopts the grinding method of liquid phase to nanocrystallize the material and modify it by doping different metal ions, so as to improve the ionic conductivity of the material and effectively improve the capacity of the material [4].

## 2. Experimental Method and Result Characterization

### 2.1. Chemical Reagents and Instruments

Table 1. Experimental drugs.

| Name                | structural formula   | Mass/g.mol <sup>-1</sup> | purity |
|---------------------|--|--------------------------|--------|
| Lithium acetate     | $\text{C}_2\text{H}_3\text{O}_2\text{Li}\cdot 2\text{H}_2\text{O}$ | 102.02                   | 99%    |
| iron nitrate        | $\text{Fe}(\text{NO}_3)_3\cdot 9\text{H}_2\text{O}$                | 404                      | 99%    |
| glucose             | $\text{C}_6\text{H}_{12}\text{O}_6\cdot \text{H}_2\text{O}$        | 198.17                   | 99%    |
| ethyl orthosilicate | $\text{C}_8\text{H}_2\text{O}_4\text{Si}$                          | 208.33                   | 99%    |
| ethanol             | $\text{CH}_3\text{CH}_2\text{OH}$                                  | 46.07                    | 95%    |
| aerosil             | $\text{SiO}_2$   | 60                       | 99%    |
| Manganese acetate   | $\text{MnAc}\cdot 4\text{H}_2\text{O}$                             | 173                      | 99%    |
| tetrabutyl titanate | $\text{C}_{16}\text{H}_{36}\text{O}_4\text{Ti}$                    | 340                      | 99%    |
| acetone             | $\text{CH}_3\text{COCH}_3$   | 58.08                    | 99%    |

Table 2. Experimental Equipment.

| Name                                       | model          | factory                                       |
|--|----------------|---|
| Electronic balance                         | XPE56          | Mettler toledo                                |
| magnetic stirrer                           | MYP19          | Shanghai Instrument Manufacturing Co., Ltd.   |
| Planetary ball mill                        | PM400          | Laichi  |
| Tube furnace                               | BTF-1200C-R    | Anhui beiyike equipment technology co., ltd   |
| Comprehensive electrochemical test system. | 1470E          | Ameike  |
| Particle size analyzer                     | Malvin 3000    | Marvin instrument co., ltd                    |
| Thermogravimetric tester                   | STA449         | Netzsch                                       |
| XRD  | D8 ADVANCE ECO | Bruker  |
| Charge and discharge tester                | XW4230         | Shenzhen xinwei new energytechnology co., ltd |

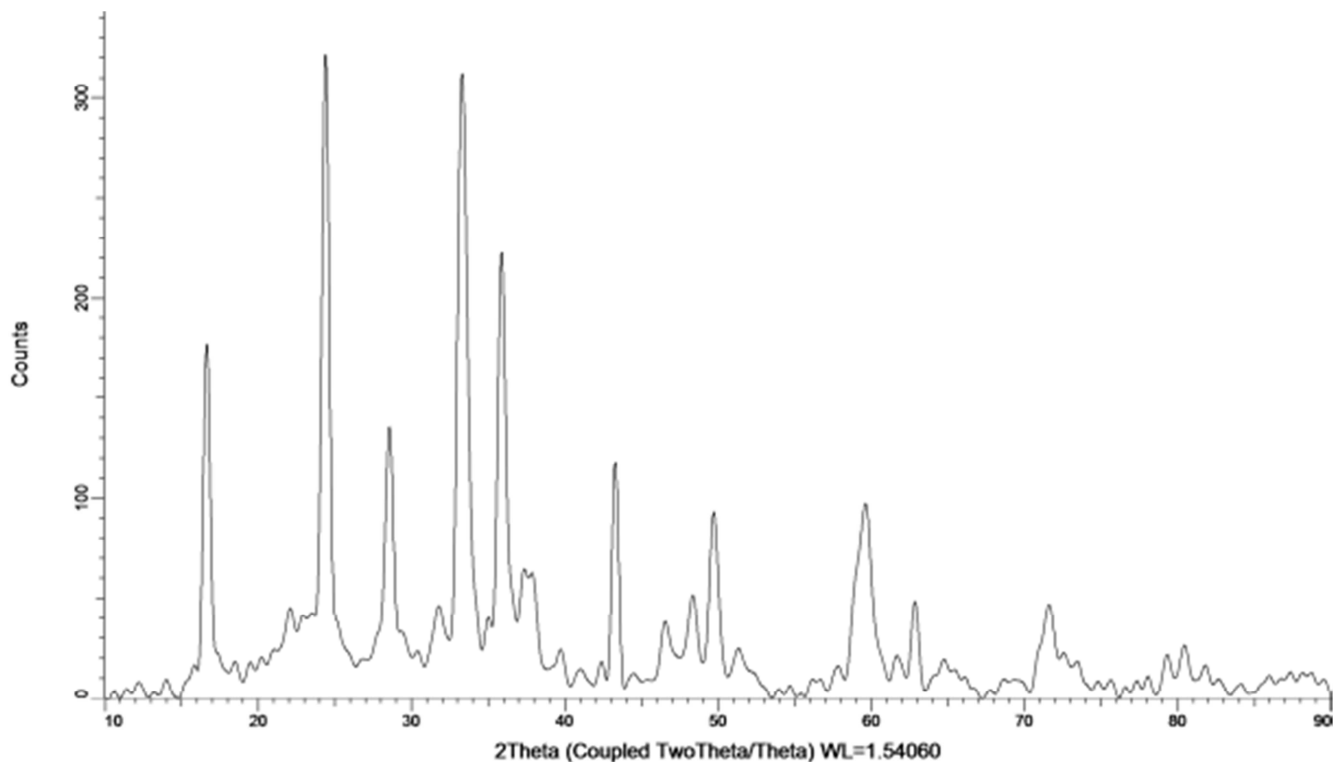


Figure 1.  $\text{Li}_2\text{FeSiO}_4$  - 100%.

## 2.2. Synthesis and Characterization

Synthetic process:

Select  $\text{LiAc}\cdot 2\text{H}_2\text{O}$  (appropriate amount),  $\text{Fe}(\text{NO}_3)_3\cdot 9\text{H}_2\text{O}$  (appropriate amount), TEOS (appropriate amount) and glucose (appropriate amount), stir and mix in ethanol solution (AR grade) for 2h; After that, it shall be dried in the oven (drying temperature is  $80^\circ\text{C}$ ) for 8h, and then the dried powder shall be taken out for curing and sintering at  $650^\circ\text{C}$  in the tubular furnace for 7h (heating rate is  $10^\circ\text{C}/\text{min}$ ) under ( $\text{N}_2/\text{Ar}_2$ ) shielding gas;  $\text{Li}_2\text{FeSiO}_4$  base material is obtained by grinding and sieving the product, and its XRD is shown in Figure 1 [5].

In order to judge the thermal stability of the material, we tested the material by TG-DSC to judge the decomposition temperature of the material [6]. The experimental results show that the starting temperature of material decomposition is  $74^\circ\text{C}$ , and it is basically completely decomposed at  $420^\circ\text{C}$ , and the exothermic temperature is basically linear. We analyze the particle size of the material. The equipment model is Marvin 3000. The particle size information can be obtained by using the

formula Stokes Einstein equation  $D = \frac{RT}{6N_A\pi\tau\sigma}$  to

represent [7], Result  $D(50) = 400\text{ nm}$ . The test results are shown in Figure 2.

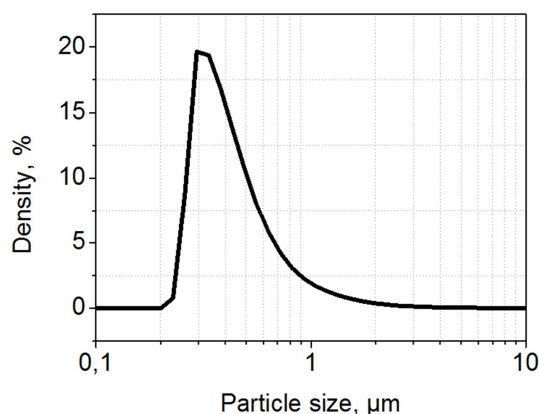


Figure 2. Particle size test.

In order to characterize the electrochemical performance of the material, a button battery was prepared. Firstly, the required material was weighed according to the mass ratio of cathode material: conductive carbon black: PVDF of 8:1:1, and then put into a ceramic mortar for dispersion and grinding. After full grinding and dispersion, an appropriate amount of NMP was added and continued grinding for a certain time. After the slurry became a certain viscosity, it was evenly coated on the collector, Then put the coated collector into a vacuum oven and place it at  $80^\circ\text{C}$  for 12 hours. Button battery CR2032 is equipped with cathode electrode. The thickness of porous polyethylene diaphragm is  $25\ \mu\text{m}$ . metal lithium sheet is assembled in argon filled glove box as negative electrode.  $\text{H}_2\text{O}\% < 1\text{ppm}$  and  $\text{O}_2\% < 50\text{ppm}$  in argon filled glove box. The electrolyte 1 mol  $\text{LiPF}_6$  solution was prepared in a mixed solvent with a volume ratio

of vinyl carbonate, dimethyl carbonate and methyl ethyl carbonate of 1:1:1. All batteries were maintained at open circuit voltage for 6 hours before electrochemical measurement [8].

Bts-hardware-ct-3008-5v10ma (xinwei, China) battery test system is used to charge and discharge the battery with a current of 0.05c in the voltage range of 1.5-4.8v (vs  $\text{Li}/\text{Li}^+$ ). The measured specific energy of the battery is 120 mAh/g [9], and the results are shown in Figure 3.

It can be seen from the test results that 100%  $\text{Li}_2\text{FeSiO}_4$  material is obtained by solid-state sintering. Through thermogravimetric analysis, its decomposition temperature is  $420^\circ\text{C}$ , showing excellent thermal stability of Si-O bond. The exothermic curve changes linearly, which is conducive to the tracking analysis of material entropy enthalpy change. The capacity is stable at 120mAh/G. through particle size measurement, the particle size  $D50 = 400\text{nm}$ , and the compaction density is low in electrode preparation, Affect the exertion and improvement of battery capacity.

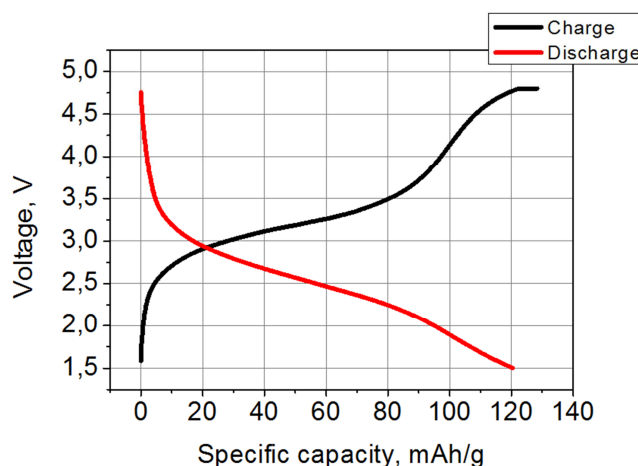


Figure 3. Charge discharge cycle test.

## 2.3. Material Nanocrystallization

In order to improve the specific surface area of the material, increase the ion exchange capacity and shorten the ion migration distance,  $\text{Li}_2\text{FeSiO}_4$  was used as the substrate, surfactant was added and gas-phase nano Si was sintered by liquid-phase grinding [10].

Synthesis process:

$\text{LiAc}\cdot 2\text{H}_2\text{O}$  (appropriate amount),  $\text{Fe}(\text{NO}_3)_3\cdot 9\text{H}_2\text{O}$  (appropriate amount), aerosil  $\text{SiO}_2$  (appropriate amount), glucose (appropriate amount), surface (for aerosol dispersion) surfactant (for aerosol dispersion) were selected, stirred and mixed in ethanol solution (AR grade), and ball milled in acetone (400 RPM) 6 hours; then curing and sintering were carried out at  $650^\circ\text{C}$  for 10 hours, and [11] was carried out under  $\text{N}_2/\text{air}_2$  shielding gas; the product was ground and screened to obtain nano-sized [ $D(50) = 15\text{ nm}$ ]  $\text{Li}_2\text{FeSiO}_4$  (90%) materials (including Fe (7%) and  $\text{Li}_2\text{SiO}_3$  (3%).

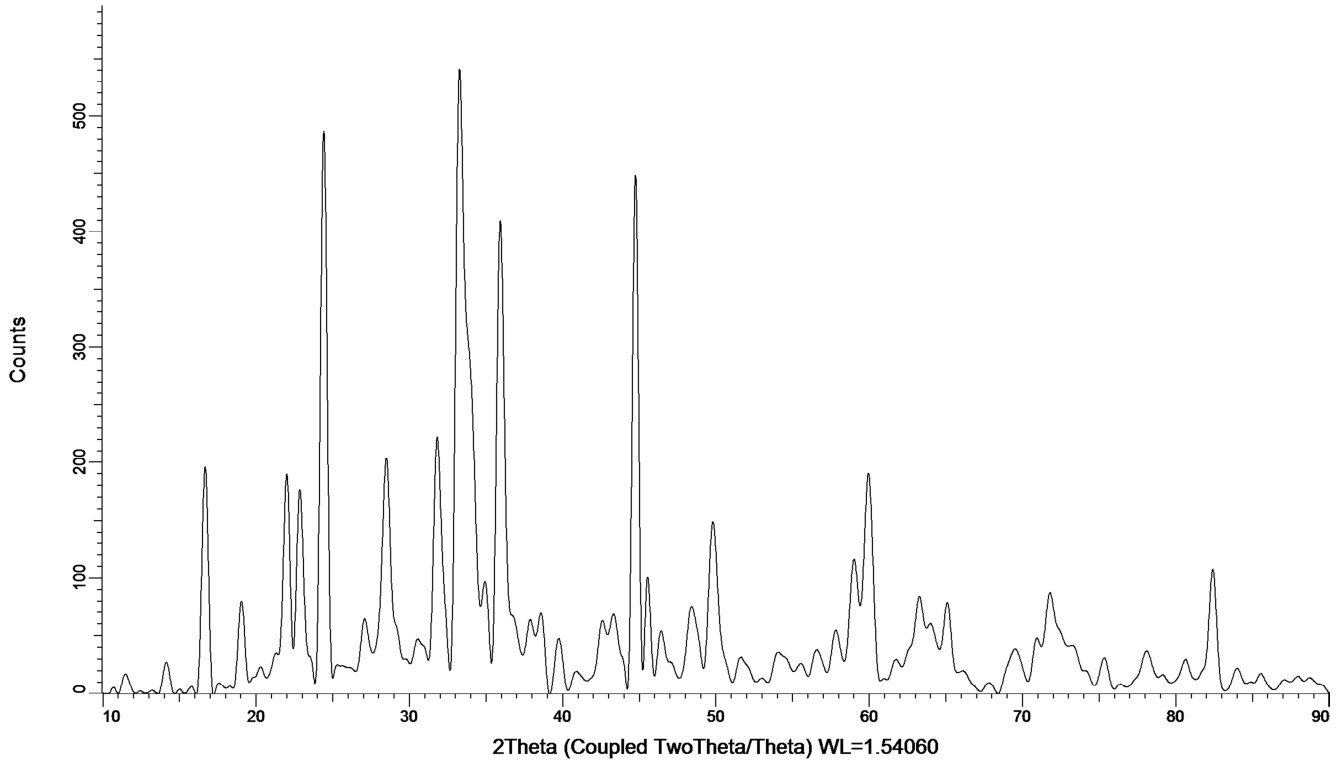


Figure 4.  $\text{Li}_2\text{FeSiO}_4$  - 90%, (Fe - 7%,  $\text{Li}_2\text{SiO}_3$ - 3%) XRD.

Nano  $\text{Li}_2\text{FeSiO}_4$  (90%) particle size distribution:

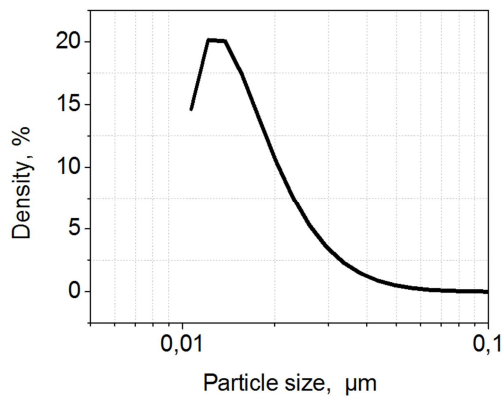


Figure 5.  $\text{Li}_2\text{FeSiO}_4$  - 90% (Fe - 7%,  $\text{Li}_2\text{SiO}_3$ - 3%) particle size distribution.

After the improved nano  $\text{Li}_2\text{FeSiO}_4$  (90%) was made into button battery, the charge discharge test was carried out according to the original conditions, and the specific energy was 140 mAh/g, as shown in Figure 5.

In conclusion, the addition of gaseous  $\text{SiO}_2$  surfactant improves the interface specific surface area of the material, improves the surface free energy combined with solvent liquid-phase grinding, and effectively improves the preparation efficiency; In the grinding process of ethanol and acetone mixture, the alcohol and ketone tautomers are in the dynamic equilibrium of ketone and enol. With the grinding time and reaction, the enol type continues to decrease and the ketone mode continues to convert to enol type. Acetone encounters positively charged metal ions to

form stable metal salts, thus stabilizing the structure of the material [12] and reducing the oxidation of Fe; After liquid phase grinding,  $\text{Li}_2\text{FeSiO}_4$  (100%), D50 = 400 nm substrate is transformed into  $\text{Li}_2\text{FeSiO}_4$  (90%), Fe (7%),  $\text{Li}_2\text{SiO}_3$  (3%), D50 = 15 nm, which not only refines the nano size of the material, but also increases the content of Fe source and  $\text{Li}_2\text{SiO}_3$  crystal lithium source, improves the specific surface area, shortens the lithium ion diffusion path and improves the ion migration rate; Because the addition of Si based materials greatly improves the thermal stability of the materials, it tends to be completely decomposed when it is greater than 500°C, and the specific energy is increased to 140mAh/g.

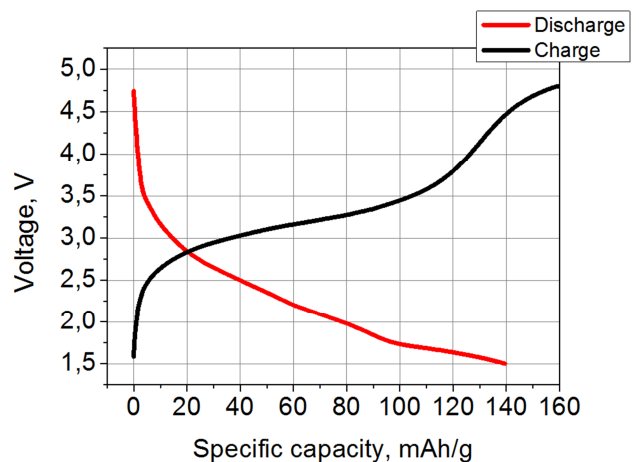


Figure 6. Charge discharge curves of  $\text{Li}_2\text{FeSiO}_4$  (90%), Fe (7%) and  $\text{Li}_2\text{SiO}_3$  (3%).

**2.4. Doping of Mn Ions (Fe: Mn ~ 1:1)**

Synthesis process:

Select  $Li_2CO_3 \cdot 2H_2O$  (appropriate amount),  $MnCl_2 \cdot 4H_2O$  (appropriate amount),  $FeC_2O_4 \cdot 2H_2O$  (appropriate amount), TEOS tetraethyl orthosilicate (appropriate amount), sucrose sucrose (appropriate amount), stir and mix in ethanol solution (AR grade), ball mill in acetone (400 rpm,

6 hours). After TEOS is diluted with ethyl alcohol, drop it at the rate of 10 ~ 20 drops/min, and then stir for 30 minutes; Curing and sintering at 650°C for - 8h ( $N_2/air_2$ ) under shielding gas;  $Li_2Fe_{0.5}Mn_{0.5}SiO_4$  was obtained by grinding and screening.

The XRD is shown in Figure 6.

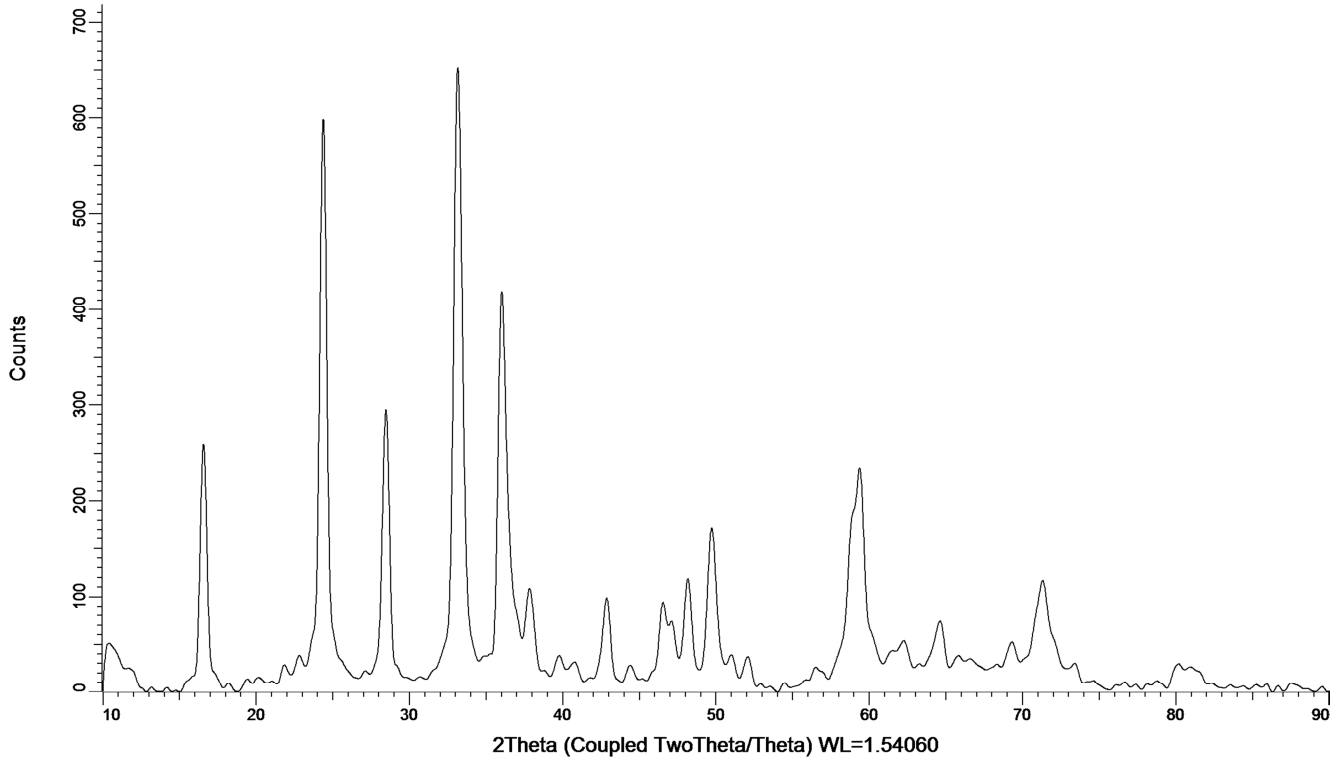


Figure 7.  $Li_2Fe_{0.5}Mn_{0.5}SiO_4$  - 100%.

It can be seen that the decomposition starting temperature of the material becomes higher, about 115°C, which increases the thermal stability of the material.

The button battery made of  $Li_2Fe_{0.5}Mn_{0.5}SiO_4$  doped with Mn ion was charged and discharged under the original conditions, and the specific energy was 160 mAh/g. The charge discharge electrogram of  $Li_2Fe_{0.5}Mn_{0.5}SiO_4$  material is shown in Figure 8.

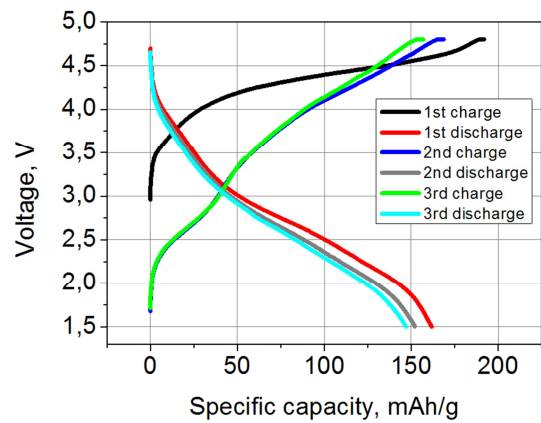


Figure 9. Charge discharge diagram of  $Li_2Fe_{0.5}Mn_{0.5}SiO_4$ .

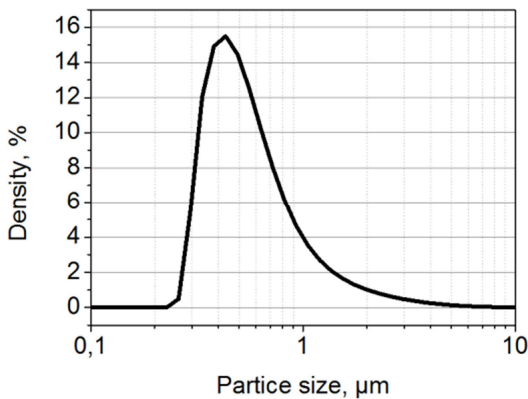


Figure 8. Particle size distribution of  $Li_2Fe_{0.5}Mn_{0.5}SiO_4$  particle size distribution  $D(50) = 500$  nm.

By analyzing the above experimental results, it will be found that with the increase of TEOS content,  $SiO_2$  formed by hydrolysis increases, which is conducive to improving the coating rate of the material [13], resulting in the gradual decrease of  $H_2$  release and the gradual increase of the coating rate of the material, which is conducive to maintaining the activity of the material; The entry of Mn ions into the positive material crystal can improve the specific energy of

the positive material, up to 160mah/g. This may be because Mn ions replace some Fe ions, change the crystal structure of the positive material, increase the embedding space of lithium ions, or reduce the transition energy level of lithium ions [14]. However, with the shuttle effect of electrochemical reaction process, the valence change of Mn ions leads to the attenuation of high-temperature stability of materials, that is, the Jahn teller effect of Mn ions can easily change their oxidation state + 2 to + 3/+ 4, which is lower than 4.8 V, just as Fe ions change their oxidation state + 2 to + 3, which is lower than 4.8 v [15]. Capacity attenuation is found after repeated cycles.

**2.5. Adding Ti, V (Fe: Ti/V ~ 10:1) Ions Increases the Stability of the Material**

Synthesis process:

LiAc·2H<sub>2</sub>O (appropriate), MnAc·4H<sub>2</sub>O (appropriate), FeC<sub>2</sub>O<sub>4</sub>·2H<sub>2</sub>O (appropriate), TEOS (appropriate), sucrose sucrose (appropriate), tetrabutyl titanate (appropriate); Stir and mix in ethanol solution (AR grade) and ball mill in acetone (400 rpm, 6 hours); Curing and sintering at 650°C for 8h, under N<sub>2</sub>/air shielding gas [16]; After grinding and screening, stable Li<sub>2</sub>Fe<sub>0.5</sub>Mn<sub>0.45</sub>Ti<sub>0.05</sub>SiO<sub>4</sub> - 82% (Li<sub>2</sub>SiO<sub>3</sub> - 18%) and its structure are shown in Figure 9.

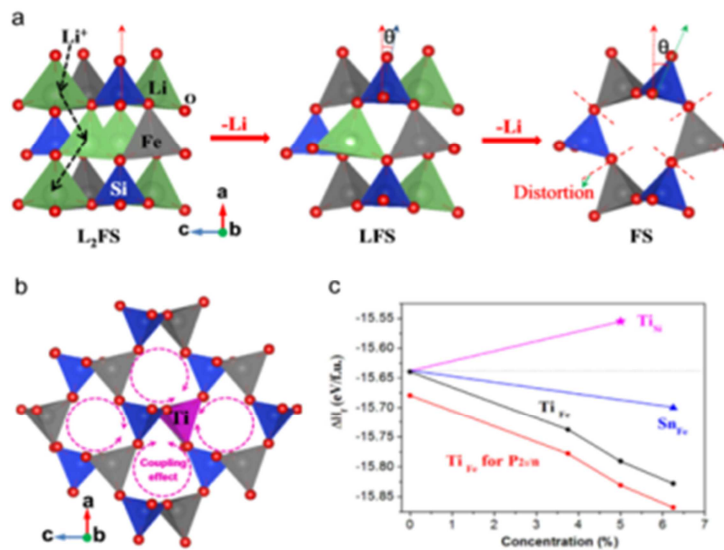


Figure 10. Li<sub>2</sub>Fe<sub>0.5</sub>Mn<sub>0.45</sub>Ti<sub>0.05</sub>SiO<sub>4</sub>.

XRD test of Li<sub>2</sub>Fe<sub>0.5</sub>Mn<sub>0.45</sub>Ti<sub>0.05</sub>SiO<sub>4</sub> material:

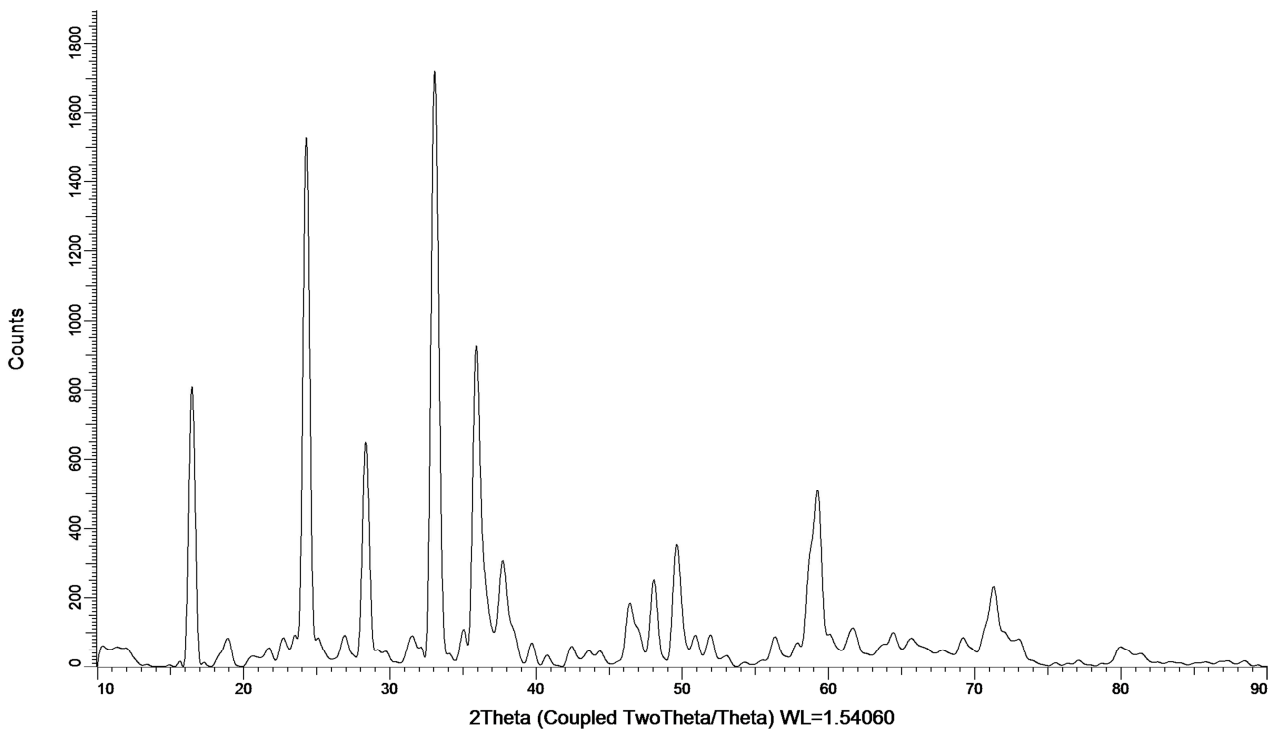
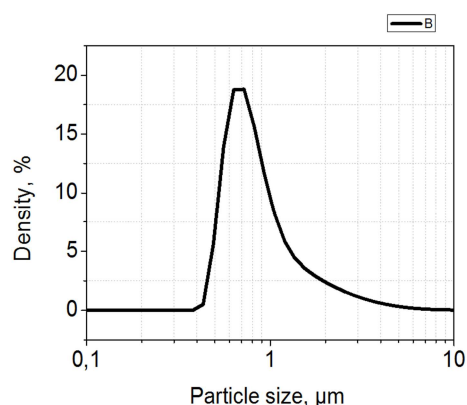


Figure 11. xrd-Li<sub>2</sub>Fe<sub>0.5</sub>Mn<sub>0.45</sub>Ti<sub>0.05</sub>SiO<sub>4</sub> - 82%, (Li<sub>2</sub>SiO<sub>3</sub> - 18%).

$\text{Li}_2\text{Fe}_{0.5}\text{Mn}_{0.45}\text{Ti}_{0.05}\text{SiO}_4$  particle size analysis:



**Figure 12.** Particle size distribution of  $\text{Li}_2\text{Fe}_{0.5}\text{Mn}_{0.45}\text{Ti}_{0.05}\text{SiO}_4$  ( $\text{Li}_2\text{SiO}_3$  - 18%)  $\text{Li}_2\text{Fe}_{0.5}\text{Mn}_{0.45}\text{Ti}_{0.05}\text{SiO}_4$ .

Material electrochemical performance test:

After the button battery was made of  $\text{Li}_2\text{Fe}_{0.5}\text{Mn}_{0.45}\text{Ti}_{0.05}\text{SiO}_4$  [ $\text{Li}_2\text{SiO}_3$  (18%)] doped with Ti and V ions, the charge discharge test was carried out under the original conditions (1.5 – 4.8 V, 0.05 C), The specific energy obtained is 190 mAh/g, and the charge discharge electrogram is shown in Figure 13.

During the preparation of  $\text{Li}_2\text{Fe}_{0.5}\text{Mn}_{0.45}\text{Ti}_{0.05}\text{SiO}_4$  ( $\text{Li}_2\text{SiO}_3$  - 18%), tetrabutyl titanate is hydrolyzed with TEOS. After hydrolysis of titanium dioxide, charged sol is obtained to improve ionic conductivity and Si-O bonding to improve high heat resistance [17]. The addition of Ti can stabilize the structure. Li, Mn and Fe source materials produce ketone reaction through liquid-phase catalytic grinding to attract metal ions to form stable metal salts.  $\text{Li}_2\text{Fe}_{0.5}\text{Mn}_{0.45}\text{Ti}_{0.05}\text{SiO}_4$  [ $\text{Li}_2\text{SiO}_3$  (18%)] is obtained through solid-phase sintering reaction. The composite powder material with good high temperature stability and D50 = 500nm is obtained through TG-DSC analysis. Through electrochemical test, its capacity reaches 190mAh/g.

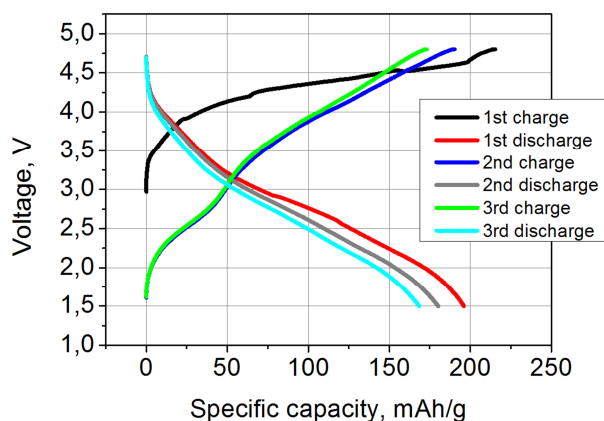


**Figure 13.** Charge discharge diagram of  $\text{Li}_2\text{Fe}_{0.5}\text{Mn}_{0.45}\text{Ti}_{0.05}\text{SiO}_4$ .

## 2.6. $\text{Li}_2\text{Fe}_{0.5}\text{Mn}_{0.5}\text{Si}_{0.975}\text{V}_{0.025}\text{O}_4 + \text{C}$ Complex Was Obtained by Doping V and C by Solid-state Synthesis

Material synthesis:

Hydrometallurgical treatment of ilmenite was carried out and atmospheric pressure leaching was carried out in hydrochloric acid to prepare the precursor of ferrous oxalate. After the leaching solution was adjusted, pH4.0 was adjusted, and excess oxalic acid was added to obtain the precipitate.

Ball milling solid phase method, feeding sequence:

Add equimolar amounts of ferrous oxalate and manganese acetate, as well as corresponding amounts of lithium silicate, lithium carbonate and corresponding proportion of  $\text{V}_2\text{O}_5$  into the ball milling tank for ball milling at 500r/min for 12h; Then calcine in  $\text{N}_2$  atmosphere at  $700^\circ\text{C}$  for 12h.

Battery preparation and testing:

Grind the cathode material  $\text{Li}_2\text{Fe}_{0.5}\text{Mn}_{0.5}\text{Si}_{0.975}\text{V}_{0.025}\text{O}_4 + \text{C}$ : Super P Li: PVDF in the ratio of 8:1:1 (by mass), dissolve the PVDF (10% solution) with nitromethyl pyrrolidone (NMP), stir and adjust the slurry, prepare the film, press, punch, vacuum dry and weigh to prepare the cathode electrode sheet, assemble the button CR2032 half cell in the glove box, and conduct the charge discharge test after placing it.

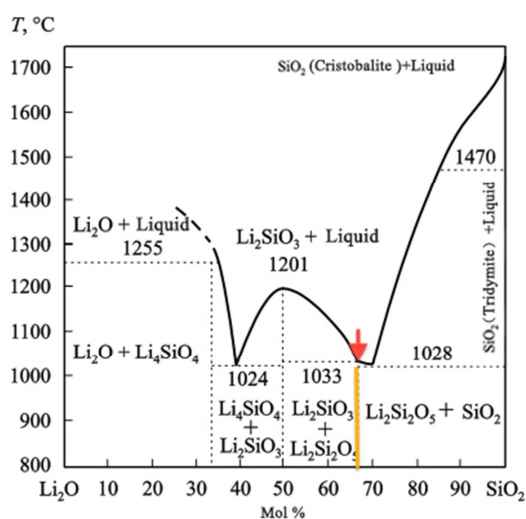


**Figure 14.** State diagram of  $\text{Li}_2\text{O}$ - $\text{SiO}_2$  system.

It can be seen from the figure that the cathode material of  $\text{Li}_2\text{FeSiO}_4$  obtains the amorphous alloy with the lowest amount of  $\text{SiO}_2$  in the  $\text{Li}_2\text{O}$ - $\text{SiO}_2$  system, and lithium is evenly distributed after crystallization. The experimental data show that the addition of oxide  $\text{V}_2\text{O}_5$  has a certain effect on the crystallization efficiency of amorphous alloy, especially for  $\text{Li}_2\text{FeSi}_{1-x}\text{M}_x$ . The multi-component compound of  $\text{O}_4$  can obtain the nanocrystalline structure by two-stage heat treatment of amorphous alloy. The compound  $\text{Li}_2\text{Fe}_{0.5}\text{Mn}_{0.5}\text{Si}_{0.975}\text{V}_{0.025}\text{O}_4$  can be obtained by doping Mn with  $\text{Li}_2\text{FeSiO}_4$  by mechanochemical synthesis. In order to improve the electrochemical performance of lithium ion battery, conductive carbon source was added to obtain nanocomposite  $\text{Li}_2\text{Fe}_{0.5}\text{Mn}_{0.5}\text{Si}_{0.975}\text{V}_{0.025}\text{O}_4 + \text{C}$  to improve the conductivity of cathode material. The liquid phase technology of  $\text{Li}_2\text{O}$ - $\text{SiO}_2$  modified amorphous alloy can achieve 100% amorphization when cooled in air. In the study of crystallization kinetics of amorphous alloy, as shown in

Figure 15, it is found for the first time that the optimal proportion of crystalline phase ( $\text{Li}_2\text{O} + 60\% \text{SiO}_2$ ) and the modification temperature point of the alloy,  $\text{V}_2\text{O}_5$  is used as a crystallization inhibitor to improve the crystal structure and phase composition of  $\text{Li}_2\text{FeSiO}_4$  which is conducive to

improving the electrochemical performance of lithium ion battery. At the same time, a mechanochemical technology doped with manganese was developed to make the yield of  $\text{Li}_2\text{Fe}_{0.5}\text{Mn}_{0.5}\text{Si}_{0.975}\text{V}_{0.025}\text{O}_4 + \text{C}$  reach 100%.

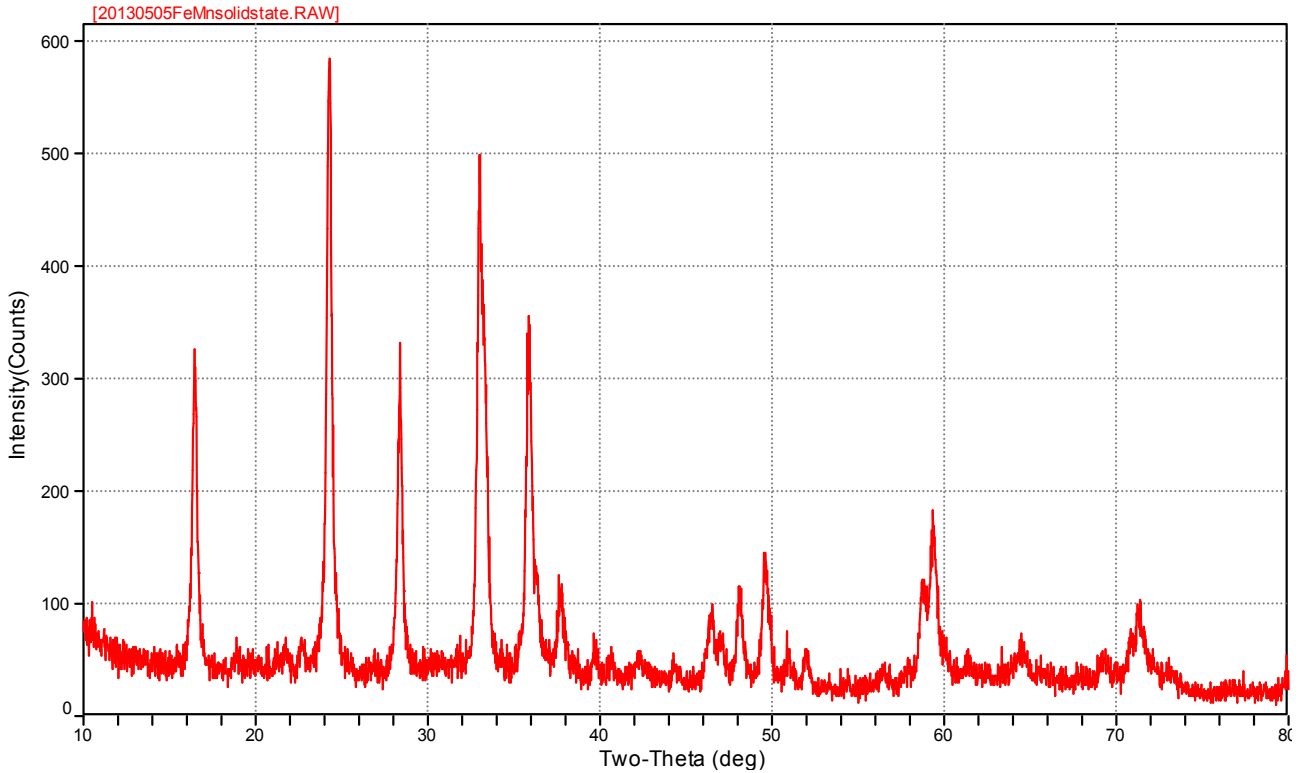


Figure 15. XRD pattern of cathode material  $\text{Li}_2\text{Fe}_{0.5}\text{Mn}_{0.5}\text{Si}_{0.975}\text{V}_{0.025}\text{O}_4 + \text{C}$ .

The synthesized cathode material belongs to 700°C - p21/N crystal phase, and a small amount of  $\text{Li}_2\text{SiO}_3$  diffraction peaks appear.

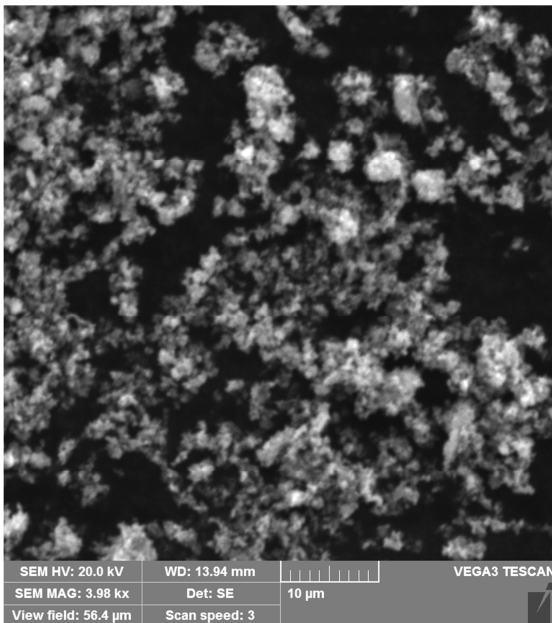


Figure 16. SEM of cathode material  $\text{Li}_2\text{Fe}_{0.5}\text{Mn}_{0.5}\text{Si}_{0.975}\text{V}_{0.025}\text{O}_4 + \text{C}$  Composite.

(particle size < 3 μm)

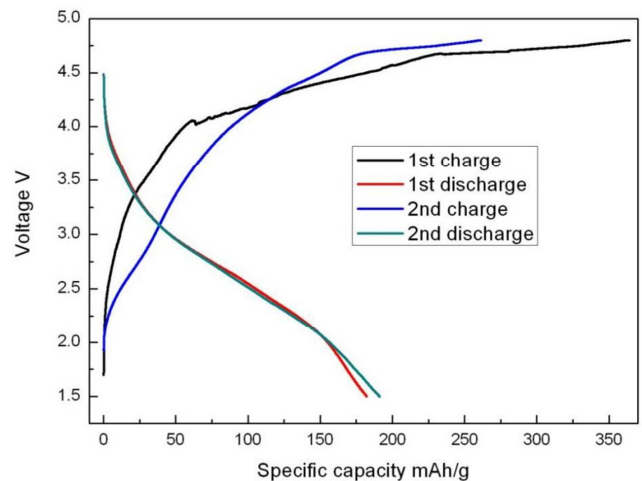


Figure 17. Charge discharge curve of cathode material  $\text{Li}_2\text{Fe}_{0.5}\text{Mn}_{0.5}\text{Si}_{0.975}\text{V}_{0.025}\text{O}_4 + \text{C}$  at 0.05c rate.

Charge 363mAh/g for the first cycle and discharge 182mAh/g for the first cycle; Charge 262mAh/g and discharge 191mAh/g in the second cycle, the voltage platform of the charging curve appears above 4.0V, and the decrease of the voltage platform in the second cycle is

smaller than that of  $\text{Li}_2\text{FeSiO}_4$ .

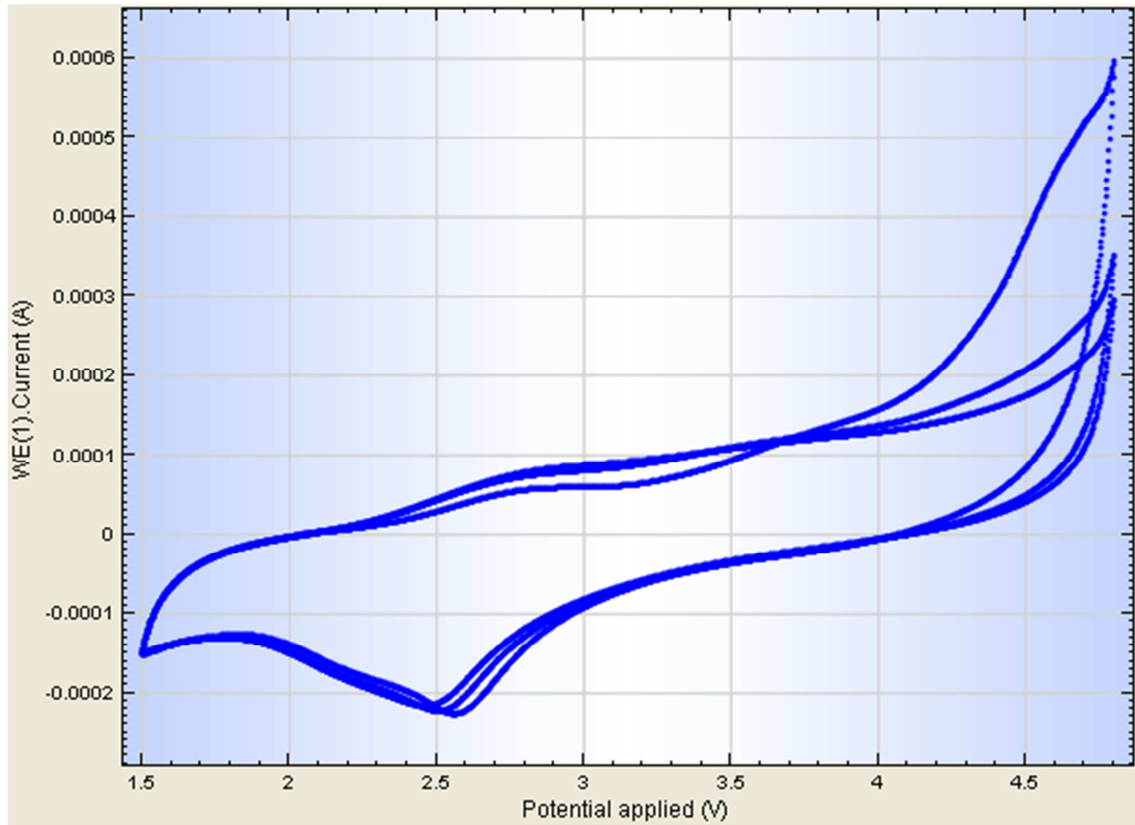


Figure 18. CV diagram of cathode material  $\text{Li}_2\text{Fe}_{0.5}\text{Mn}_{0.5}\text{Si}_{0.975}\text{V}_{0.025}\text{O}_4/\text{c}$  composite electrode at 1mV/S.

It can be seen that  $\text{Li}_2\text{Fe}_{0.5}\text{Mn}_{0.5}\text{Si}_{0.975}\text{V}_{0.025}\text{O}_4 + \text{C}$  is synthesized by using ferrous oxalate synthesized from ore as precursor, adding elements Ti and V, grinding and coating with C source added by solid-state synthesis sintering combined with mechanochemical method, and the material particles are small ( $< 3 \mu\text{m}$ ) It has no magnetism. At the rate of 0.05c, the first charge is up to 360mah/g, the second charge is up to 292 mAah/g, the reversible specific discharge capacity is 190mAh/g, and the average coulomb efficiency is 73%, which is low.

It can be seen from the figure that the charging capacity of  $\text{Li}_2\text{FeSiO}_4$  is 130mah/g, the discharge capacity is 100mAh/g, and the efficiency is 77%. The charge discharge capacity of similar nano compounds increased and the efficiency increased to 89%. The capacity of coated carbon source ( $\text{Li}_2\text{FeSiO}_4 + \text{C}$ ) is improved, charging 175 mAh/g and discharging 140 mAh/g. Further doped with manganese, the charging capacity of titanium and vanadium  $\text{Li}_2\text{Fe}_{0.5}\text{Mn}_{0.5}\text{Si}_{0.975}\text{V}_{0.025}\text{O}_4 + \text{C}$  increased to 335mah/g and the discharge capacity was 193mAh/g.

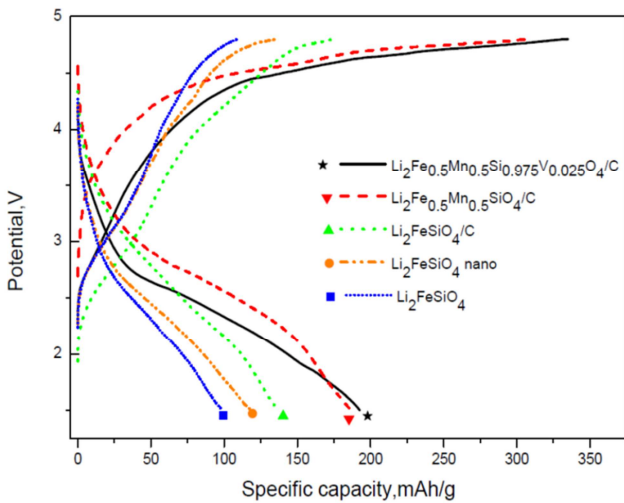


Figure 19. Effect of doped elements on electrochemical properties.

### 3. Conclusion

The  $\text{Li}_2\text{FeSiO}_4$  reference material [D (50) =400nm] prepared by sol-gel method combined with solid-phase sintering has good thermal stability and electrical conductivity  $\sim 6. \times 10^{-14} \text{ s/cm}$ , and the battery capacity prepared with this material is 120mAh/g.

When the material is synthesized, the surfactant vapor phase  $\text{SiO}_2$  is added and grinded by the liquid phase of the mixed solution of ethanol and acetone, the volatile enol type is continuously reduced, the ketone mode is continuously transformed into enol type, and acetone and positively charged metal ions form stable metal salts, so as to stabilize the structure of the material; At the same time, it will bring changes in the composition and nano size of the material, that is,  $\text{Li}_2\text{FeSiO}_4$  (100%) is transformed into  $\text{Li}_2\text{FeSiO}_4$  (90%), Fe (7%),  $\text{Li}_2\text{SiO}_3$

(3%), D (50) = 15 nm, 140mAh/g, so as to enhance the surface activity of the material and increase the specific energy.

Adding Mn source material and Mn ions into the positive material crystal can improve the specific energy of the material, and its mechanism needs to be further discussed. Using TEOS, with the increase of its content, SiO<sub>2</sub> formed by hydrolysis increases, which is conducive to improve the coating rate of the material, resulting in the gradual decrease of H<sub>2</sub> release and the gradual increase of the coating rate of the material, which is conducive to the acquisition of active Li<sub>2</sub>Fe<sub>0.5</sub>Mn<sub>0.5</sub>SiO<sub>4</sub> [LF(M)s] (d (50) = 500 nm, 160 mAh/g), but due to the electrochemical reaction shuttle effect, the cycle stability is reduced, and the capacity attenuation is accelerated after multiple cycles. For LF (m) S doping treatment of Ti ion helps to improve the internal structure of the material. Tetrabutyl titanate hydrolyzes with TEOS. After hydrolysis of titanium dioxide, charged sol crosslinks are obtained to improve ionic conductivity and Si-O bonding to improve high heat resistance, Li, Mn and Fe source materials are ground by liquid phase catalysis to produce keto enol reaction to form stable metal salt. High temperature stable D (50) = 500nm, Li<sub>2</sub>Fe<sub>0.5</sub>Mn<sub>0.45</sub>Ti<sub>0.05</sub>SiO<sub>4</sub> [Li<sub>2</sub>SiO<sub>3</sub> (18%)] composite powder is obtained by solid-phase sintering reaction, and its capacity can reach 190mAh/g.

The research shows that further optimization of LF (m) s and D (50) = 500nm is expected to further improve the specific energy. In addition, Li<sub>2</sub>Fe<sub>0.5</sub>Mn<sub>v0.5</sub>SiO<sub>4</sub> + C is obtained by C coating combined with mechanochemical method, which improves the ionic conductivity of the material, and greatly improves the charging efficiency of the material, so that it reaches 360mAh/g and the discharge reaches 190mAh/g. it can be seen that the composite LF (m) There is still room for capacity improvement in S + C, and some necessary exploration is still needed.

## References

- [1] Z. Li, J. Huang, B. Y. Liaw, V. Metzler, J. Zhang, *Journal of Power Sources* 245 (2014) 168-182.
- [2] Popovich A. A., Maximov M. Yu., Rumyantsev A. M., Novikov P. A. *Russian Journal of Applied Chemistry*, 2015, 88 (5), 898-899.
- [3] Popovich, A. A., Maximov, M. Y., Novikov, P. A., Silin, A. O., Nazarov, D. V., Rumyantsev, A. M. *Russian Journal of Applied Chemistry*, 2016, 89 (4), 679-681.
- [4] Wang, Q.-S., Popovich, A. A., Bao, Y.-Y., Novikov P. A., Zheng, L.-Y., Razumov N. G., Yang Z.-L., Silin A. O. *Journal of Functional Materials*, 2014, 45 (13), 13098-13101+13107.
- [5] Popovich, A. A., Novikov, P. A., Silin, A. O., Razumov, N. G., Sheng, W. Q. *Russian Journal of Applied Chemistry*, 2014, 87 (9), 1268-1273.
- [6] Konstantin Pushnitsa, Pavel Novikov, Anatoly Popovich, Qingsheng Wang. *Advanced Materials Research*, 2015, 1120-1121, 132-136. [https://www.arb.ca.gov/msprog/bus/battery\\_cost.pdf](https://www.arb.ca.gov/msprog/bus/battery_cost.pdf)
- [7] Armand, M., & Tarascon, J.-M. (2008). Building better batteries. *Nature*, 451 (7179), 652–657.
- [8] R. Murugan, V. Thangadurai, W. Weppner. *Angewandte Chemie Int. Ed. Engl.*, 2007, 46, 7778-7781. Web source: <https://www.mindat.org/min-1651.html>
- [9] H. M. Kasper, *Inorg. Chem.*, 1969, 8 (4), 1000–1002.
- [10] Y. Chen, E. Rangasamy, C. Liang, K. An *Chemistry of Materials*, 2015, 27 (16), 5491–5494.
- [11] R. Murugan, V. Thangadurai, W. Weppner, *Angewandte Chemie International Edition* 2007, 46 (41), 7778-81.
- [12] J. Awaka, A. Takashima, K. Kataoka, N. Kijima, Y. Idemoto, H. Hayakawa, J. Akimoto, *Chemistry Letters*, 2011, 40 (1), 60-62.
- [13] J. Percival, P. R. Slater, *Solid State Community* 2007, 142, 355-357.
- [14] M. P. O'Callaghan, A. S. Powell, J. J. Titman, G. Z. Chen, E. J. Cussen, *Chem. Mater.* 2008, 20, 2360.
- [15] J. Percival, D. Apperley, P. R. Slater, *Solid State Ionics* 2008, 179, 1693.
- [16] J. L. Allen, J. Wolfenstine, E. Rangasamy, J. Sakamoto, *J. Power Sources* 2012, 206, 315–319.
- [17] S. Mukhopadhyay, T. Thompson, J. Sakamoto, A. Huq, J. Wolfenstine, J. L. Allen, N. Bernstein, D. A. Stewart, M. D. Johannes, *Chem. Mater.* 27 (2015) 3658–3665.